JOURNAL OF Materials CHEMISTRY

Synthesis of highly active tungsten(VI) oxide photocatalysts for oxygen evolution by hydrothermal treatment of aqueous tungstic acid solutions

Hiroshi Kominami,*[a] Kei-ichi Yabutani,[a] Takuhei Yamamoto,[a] Yoshiya Kera[a] and Bunsho Ohtani[b]

[a]*Department of Applied Chemistry, Faculty of Science and Engineering, Kinki University, Kowakae, Higashiosaka, Osaka, 577-8502, Japan. E-mail: hiro@apch.kindai.ac.jp*
[b]*Catalysis Research Center, Hokkaido University, Sapporo 060-0811, Japan*

Received 15th May 2001, Accepted 11th September 2001
First published as an Advance Article on the web 25th October 2001

Tungsten(VI) oxide (WO_3) powders of monoclinic crystal structure with high crystallinity have been synthesized by hydrothermal treatment (HTT), at 523 or 573 K, of aqueous tungstic acid (H_2WO_4) solutions prepared from sodium tungstate by ion-exchange (IE) with a proton-type resin. HTT and/or calcination of home-made and commercial H_2WO_4 solids of tungstite structure also produced WO_3. These WO_3 powders with various physical properties were used as photocatalysts for evolution of oxygen (O_2) from an aqueous silver sulfate solution, and the correlation between their physical properties and photocatalytic activity was examined. WO_3 powders of high crystallinity, *e.g.*, IE-HTT-WO_3 synthesized at 573 K, gave the highest O_2 yield, suggesting that the crystallinity of WO_3 is a key factor in its high activity for this reaction system. Calcination at <1073 K improved the crystallinity of some WO_3 powders, resulting in increases in their activities; however, calcination at a higher temperature reduced the activity, presumably due to formation of oxygen vacancies acting as recombination centers.

Introduction

Tungsten(VI) oxide (WO_3), the band gap energy of which has been estimated to be 2.5 eV, has the potential ability to photocatalyze reactions under irradiation of visible light of wavelength $<ca.$ 500 nm. Visible light-induced water splitting has been reported using WO_3 powder and iron(III) ions (or silver ions) as the electron acceptor.[1–4] However, commercially available WO_3 powders have been used in these studies, and the properties of WO_3 suitable for the photocatalytic activity for oxygen (O_2) evolution have not been clarified. Photocatalytic O_2 evolution, a half reaction of stoichiometric water decomposition, is not mechanistically fully understood in this process, and therefore, investigations on the visible light-induced evolution of O_2 on WO_3 are needed for, *e.g.*, development of solar energy conversion systems.

Photocatalysis of titanium(IV) oxide (TiO_2) and its possible environmental applications have been extensively studied.[5–8] In most such studies, commercial Degussa P-25 TiO_2 was used since it exhibits relatively high photocatalytic activity in various reaction systems. Therefore, there have been few reports on the correlation between physical properties and photocatalytic activity. We have reported that nano-crystalline TiO_2 can be synthesized by the HyCOM (Hydrothermal Crystallization in Organic Media) method and that a wide range of physical properties, *e.g.*, crystallinity and surface area, can be controlled by post-calcination.[9,10] We examined the correlations between physical properties and photocatalytic activities of HyCOM TiO_2 in several reaction systems.[11–14] In O_2 evolution from an aqueous suspension of TiO_2 powders, TiO_2 of higher crystallinity exhibited higher activity, suggesting that recombination of a photogenerated electron–hole pair (e^-–h^+) is a decisive factor in this system.[11,12]

Based on the results of HyCOM TiO_2, it is expected that WO_3 of high crystallinity would exhibit higher activity in an O_2 evolution system. In this study, we used a new method for synthesizing WO_3 powders of high crystallinity, *i.e.*, hydrothermal treatment (HTT) of an aqueous tungstic acid (H_2WO_4) solution that is prepared from sodium tungstate (Na_2WO_4) by cation-exchange using an ion-exchange (IE) resin. For comparison, WO_3 samples were also prepared by HTT and/or calcination of home-made and commercial H_2WO_4 precursors. By examining the photocatalytic activities of various WO_3 samples, a correlation between photocatalytic activity and physical properties was established.

Experimental

Preparation of H_2WO_4 solutions

Aqueous H_2WO_4 solutions were prepared by the cation-exchange method with a strongly acidic IE resin in its proton (H^+) form.[15] Prior to IE, dilute hydrochloric acid (HCl) (0.1 mol dm^{-3}, 240 cm^3) was added to the resin (Organo, Amberlite IR120B NA, 30 cm^3) packed in a glass column to convert it to the H^+ form and then the resin was washed with distilled water until chloride ions were no longer detected in the eluent. An aqueous solution of Na_2WO_4 (Wako; 0.39 mol dm^{-3}, 37.5 cm^3) was loaded on the column and H_2WO_4 was recovered from the column by elution with distilled water (37.5 cm^3). The concentration of the resulting H_2WO_4 solution (75 cm^3) was determined to be 0.19 mol dm^{-3}, which corresponds to 98% recovery.

HTT and calcination

The clear H_2WO_4 solution in a glass tube was placed in a 300 cm^3 autoclave and the gap between the tube and inside wall of the autoclave was filled with 25 cm^3 of water. The autoclave was thoroughly purged with nitrogen, heated to a desired temperature (473–573 K) at a rate of 2.5 K min^{-1}, and kept at

 DOI: 10.1039/b104223h

that temperature for 2 h. After the heating, the resulting powder was washed repeatedly with acetone and dried in air at room temperature. HTT treatment of the other solid precursors was also carried out under conditions similar to those described above. Calcination of the samples was carried out in a box furnace; the sample in a combustion boat was heated to the desired temperature at a rate of 10 K min^{-1} and kept at that temperature for 1 h.

Characterization

Powder X-ray diffraction (XRD) with Cu-Kα radiation was recorded on a Rigaku RINT 2500 diffractometer equipped with a carbon monochromator. Thermogravimetry (TG) and differential thermal analysis (DTA) were performed using a Rigaku TG-8120 under a flow of air at 100 cm^3 min^{-1}. The morphology of the powders was observed using a JEOL 5200 scanning electron microscope (SEM) and a JEOL JEM-3010 transmission electron microscope (TEM). Diffuse reflectance spectra were obtained on a Shimadzu UV-2400 UV-vis spectrometer equipped with a diffuse reflectance measurement unit (ISR-2000) and recorded after Kubelka–Munk analysis. Specific surface areas were determined by the BET single-point method using nitrogen uptake at 77 K.

Photocatalytic O_2 evolution from silver sulfate in an aqueous suspension of WO_3 under deaerated conditions

Photocatalytic evolution of O_2 from silver sulfate (Ag_2SO_4) in an aqueous suspension of TiO_2 has been extensively studied.[11,12,16–22] The experimental procedure in these studies was used for the evaluation of the photocatalytic activity of WO_3. A WO_3 powder sample (50 mg) was suspended in an aqueous Ag_2SO_4 solution (250 μmol Ag^+; 5.0 cm^3) in a glass tube, purged with argon (Ar) for at least 30 min, and then sealed off with a rubber stopper. The suspension was photoirradiated with a 400 W high-pressure mercury arc at wavelength of >300 nm at 298 K under magnetic stirring (1000 rpm). A cut-off filter (Asahi Techno Glass, L-42) was used to eliminate ultraviolet radiation from the arc when the photocatalytic reaction under visible light irradiation was examined. After the irradiation, the amount of liberated O_2 was measured using a gas chromatograph. The Ag-deposited catalyst was recovered by centrifugation, washed repeatedly with distilled water, and dried overnight at 353 K. The photodeposited Ag was dissolved in concentrated nitric acid and measured by inductively coupled plasma (ICP) emission spectroscopy (Shimadzu ICPS-1000III).

Results and discussion

Synthesis of WO_3 and tungstite by HTT and calcination

Fig. 1 shows XRD patterns of the powders obtained by HTT at various temperatures (T_{HTT}) of H_2WO_4 solutions. Hydrated WO_3 ($WO_3{\cdot}0.33H_2O$)[23] was obtained by HTT at 473 K, while WO_3 with monoclinic structure[24] was obtained at 523 K (WO_3-A), suggesting that WO_3 was produced *via* $WO_3{\cdot}0.33H_2O$ during HTT. For WO_3-A, the yield of WO_3 was estimated to be 94% on the basis of the molar amount of H_2WO_4 in the feed. Further increase in T_{HTT} up to 573 K and prolongation of HTT time (t_{HTT}) at this temperature increased the crystallinity of the WO_3 products (WO_3-B and -C, respectively) due to the higher solubility of tungsten species in water at higher T_{HTT}. As clearly shown in the XRD patterns, the intensities of the 020, 200, 202, 220, 400 and 402 diffraction peaks in these products increased with T_{HTT} up to 573 K, indicating that the growth of WO_3 crystallite proceeded along the *a* and *b* axes, especially the *a* axis, under HTT conditions at 573 K. SEM photographs of $WO_3{\cdot}0.33H_2O$, WO_3-A, WO_3-B and WO_3-C samples are shown in Fig. 2. The $WO_3{\cdot}0.33H_2O$ sample consisted of

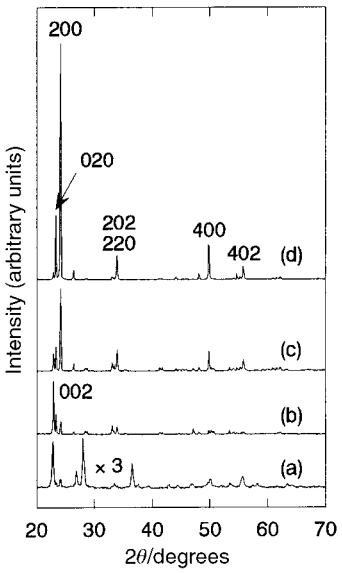

Fig. 1 XRD patterns of the compounds obtained by HTT of an H_2WO_4 solution at (a) 473 K for 2 h, (b) 523 K for 2 h (WO_3-A), (c) 573 K for 2 h (WO_3-B) and (d) 573 K for 8 h (WO_3-C).

agglomerates of fine particles, whereas WO_3-A was composed of rectangular-shaped particles. This different morphology suggests that WO_3 was formed by a dissolution–recrystallization (DR) mechanism under HTT conditions. Higher T_{HTT} and longer t_{HTT} accelerated particle growth of WO_3, and the crystalline particles of WO_3 became longer, consistent with the results of XRD. Another feature of the WO_3 particles observed in the SEM analyses was their increased coagulation at higher t_{HTT}. The BET surface area (S_{BET}) of each sample is shown in Table 1. With elevation in T_{HTT} and increased t_{HTT}, S_{BET} of WO_3 decreased due to an increase in the size of primary WO_3 particles. When the initial concentration of H_2WO_4 was increased to 0.38 mol dm^{-3}, twice that in the standard procedure described in the experimental section, gelation, *i.e.*, polymerization of H_2WO_4, occurred immediately after IE. HTT of this gel at 573 K also produced crystalline WO_3 (WO_3-F).

When the H_2WO_4 solution of the standard concentration was aged at room temperature for 24 h, a yellow solid was obtained. XRD analysis (Fig. 3(a)) revealed that this was crystalline H_2WO_4 ($WO_3{\cdot}H_2O$) in a tungstite structure[25] (designated as "Tungstite-A"). The weight loss (7.35%) observed in the TG curve from room temperature to 1273 K was almost equal to the calculated loss (7.20%) from H_2WO_4 to WO_3. HTT of Tungstite-A at 523 and 573 K also yielded crystalline WO_3 (WO_3-D and -E (Fig. 3(b)), respectively). SEM photographs of Tungstite-A, WO_3-D and WO_3-E are shown in Fig. 4. Tungstite-A consisted of plate-like particles. The morphology of WO_3-D was similar to that of the starting Tungstite-A. However, its S_{BET} (12 m^2 g^{-1}) was *ca.* three times that of the starting Tungstite-A (3.8 m^2 g^{-1}), which could not be explained by particle size effect and suggested a porous structure of WO_3-D. It is expected that formation of this WO_3 from Tungstite-A by HTT at 523 K occurs *via* intra-particle, rather than inter-particle, dehydration. Water (H_2O) molecules escaping from the tungstite crystallites would produce pores in the WO_3 particles. HTT at 573 K increased the particle size of WO_3-E and decreased S_{BET} to 1.7 m^2 g^{-1}. At 573 K, the DR mechanism was predominant, resulting in collapse of pores of WO_3 or densification of WO_3. An XRD pattern of a commercial H_2WO_4 solid (Kanto Chemicals supplied as tungstic acid) was identical to that of tungstite (designated by "Tungstite-B"). HTT of Tungstite-B at 573 K also produced WO_3 (WO_3-G). SEM photographs (Fig. 5) showed that the

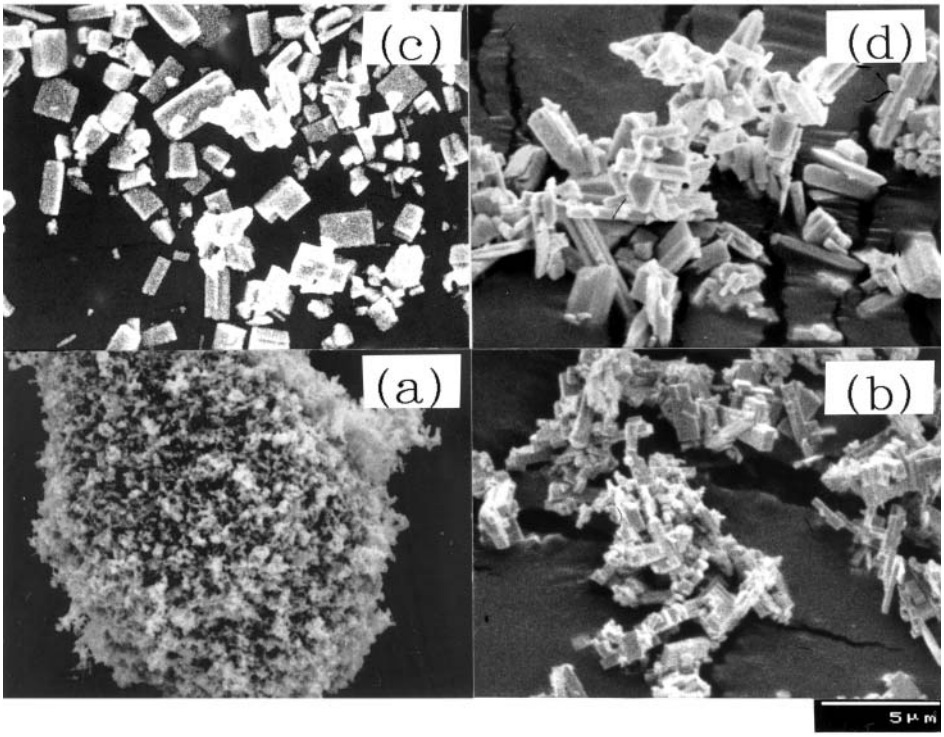

Fig. 2 SEM photographs of the compounds whose XRD patterns are shown in Fig. 1.

Tungstite-B particles were a bulky mass and WO_3-G after HTT at 573 K was composed of fine particles. The relatively large S_{BET} of WO_3-G (8.9 $m^2\,g^{-1}$) suggests that densification of WO_3 from the bulky mass of Tungstite-B was insufficient even by HTT at 573 K, in contrast to the examples of WO_3 formation from H_2WO_4 solution or Tungstite-A.

Calcination of Tungstite-B at 823 K induced its transformation into WO_3. With elevation of calcination temperature (T_C), the XRD peaks of WO_3 became sharper and S_{BET} of the products decreased as shown in Fig. 6, indicating that the WO_3 crystallites became larger upon calcination, *i.e.*, the crystallinity of WO_3 was improved gradually. Photoabsorption spectra of these WO_3 samples are shown in Fig. 7. For comparison, a spectrum of WO_3-B obtained by IE-HTT at 573 K is also shown. The absorption edge of the WO_3 samples shifted to a longer wavelength upon calcination. The shift, presumably due to an increase in their particle size,[7] was relatively small upon calcination at <973 K, while a large shift was observed upon calcination at $\geqslant 1073$ K along with a slight increase in the base line. The color of the WO_3 samples obtained by calcination at $\leqslant 973$ K was lemon-yellow, but that of the WO_3 samples calcined at $\geqslant 1073$ K was light green. Formation of oxygen vacancies in WO_3 under severe calcination conditions may account for the large shift and change in the color.[26] WO_3-B exhibited a sharper rise in absorption from the edge (*ca.* 450 nm) compared with those of the WO_3 samples prepared by calcination of Tungstite-B. This finding suggested that WO_3-B consists of large particles with few oxygen vacancies.

Photocatalytic evolution of O_2 from Ag_2SO_4 in an aqueous suspension of WO_3 under deaerated conditions

Fig. 8 shows the time course of O_2 evolution from a suspension of WO_3-B particles under UV–visible light irradiation. In this system, O_2 evolved linearly with irradiation time up to 20 min. The yields of O_2 and photodeposited Ag after 20 min irradiation were 23 and 89 μmol, respectively, and the $Ag/4O_2$ ratio was 0.97, indicating that O_2 evolution accompanying stoichiometric Ag deposition ($4Ag^+ + 2H_2O \rightarrow 4Ag + O_2 + 4H^+$) proceeds efficiently. The rate of O_2 evolution, *i.e.*, the slope of the time-course curve, gradually decreased after 20 min. The pH of the suspension decreased with the above

Table 1 Photocatalytic activity (20 min irradiation) of HT-WO_3 products prepared from various starting materials

Sample	H_2WO_4 material	T_{HTT}[a]/K	t_{HTT}[a]/h	Phase	S_{BET}/$m^2\,g^{-1}$	O_2/μmol	Ag/μmol	$Ag/4O_2$
$WO_3{\cdot}0.33H_2O$	Solution[b]	473	2	Orthorhombic	18	1.9	8.2	1.1
WO_3-A	Solution[b]	523	2	Monoclinic	14	9.6	36	0.94
WO_3-B	Solution[b]	573	2	Monoclinic	1.7	23	89	0.97
WO_3-C	Solution[b]	573	8	Monoclinic	0.6	15	58	0.97
WO_3-D	Solid,[c] Tungstite-A	523	2	Monoclinic	12	14	53	0.95
WO_3-E	Solid,[c] Tungstite-A	573	2	Monoclinic	1.7	13	55	1.1
WO_3-F	Gel[d]	573	2	Monoclinic	1.3	16	57	0.89
WO_3-G	Solid,[e] Tungstite-B	573	2	Monoclinic	8.9	3.0	13	1.1
WO_3-H[f]				Monoclinic	3.0	11	47	1.1
WO_3-I[g]				Monoclinic	3.1	9.8	41	1.0
WO_3-J[h]				Monoclinic	5.0	6.5	25	0.96
(P-25 TiO_2)[i]				Anatase, rutile	50	4.3	19	1.1

[a]Hydrothermal treatment was carried out at temperature T_{HTT} for time t_{HTT}. [b]0.19 mol dm^{-3}, 75 cm^3. [c]Prepared by aging a H_2WO_4 solution (0.19 mol dm^{-3}) at room temperature for 24 h. [d]Prepared from an H_2WO_4 solution (0.38 mol dm^{-3}) at room temperature after ion-exchange. [e]Supplied as tungstic acid from Kanto Chemicals. [f]High Purity Chemicals (99.99% purity). [g]Kishida Chemicals (99.9% purity). [h]Kanto Chemicals (99.5% purity). [i]Degussa.

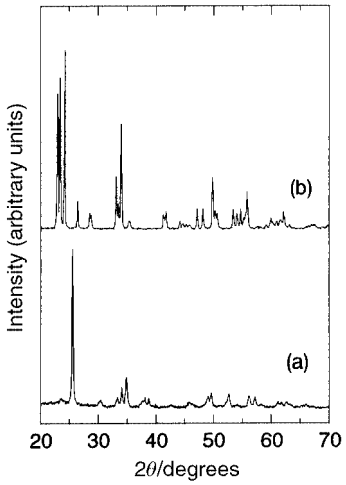

Fig. 3 XRD patterns of the compounds (a) obtained by aging of an H_2WO_4 solution for 24 h (Tungstite-A) and (b) obtained by HTT of Tungstite-A at 573 K (WO_3-E).

reaction producing H^+, and the amount of Ag^+ adsorbed on the photocatalyst particles decreased with lowering of pH,[16,17] which accounts for the decrease in O_2 evolution. The activities of the present WO_3 samples were evaluated by the yields of O_2 and Ag after 20 min irradiation and are listed in Table 1. All

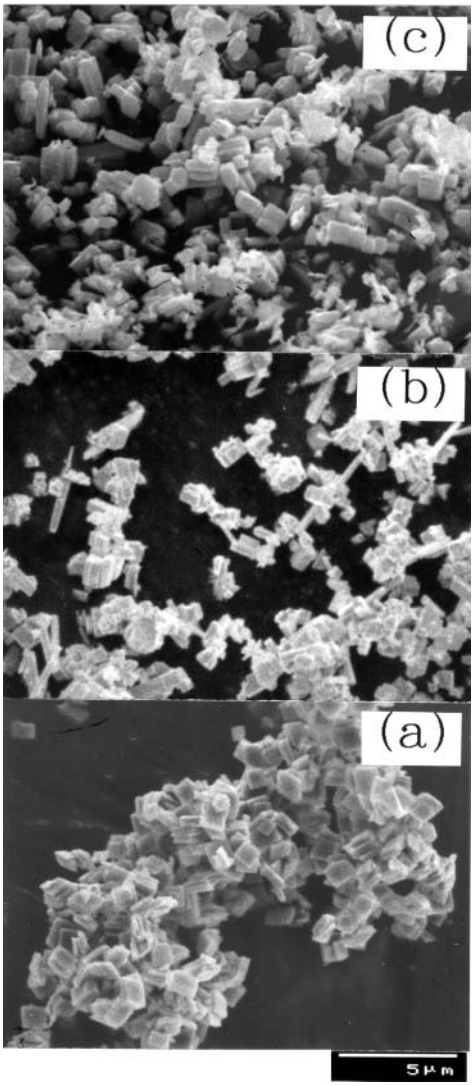

Fig. 4 SEM photographs of (a) Tungstite-A, (b) the compound obtained by HTT of Tungstite-A at 523 K (WO_3-D) and (c) WO_3-E.

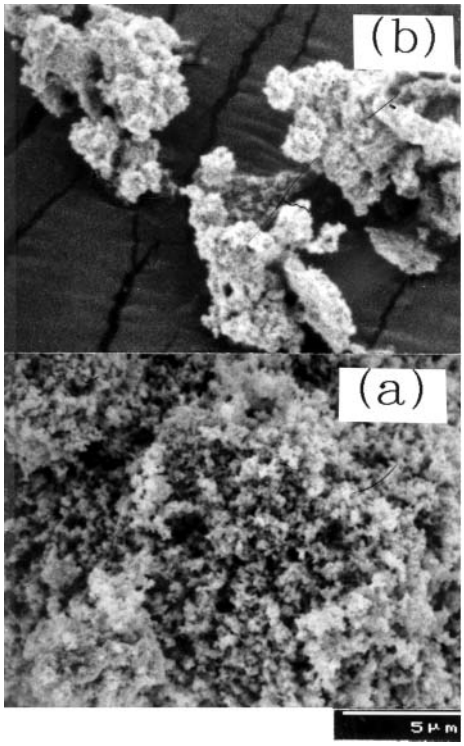

Fig. 5 SEM photographs of (a) commercial H_2WO_4 solid (Tungstite-B) and (b) the compound obtained by HTT of Tungstite-B at 573 K (WO_3-G).

WO_3 samples, including three commercial ones, tested in this study exhibited activity, though those of the tungstite and $WO_3 \cdot 0.33H_2O$ samples were negligible. Among the WO_3 samples listed in Table 1, those of high crystallinity prepared

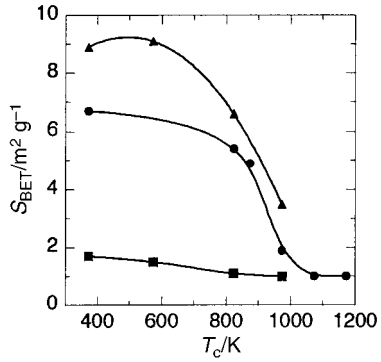

Fig. 6 Effects of calcination temperature on S_{BET} of WO_3-B (■), WO_3-G (▲), and WO_3 derived from Tungstite-B (●).

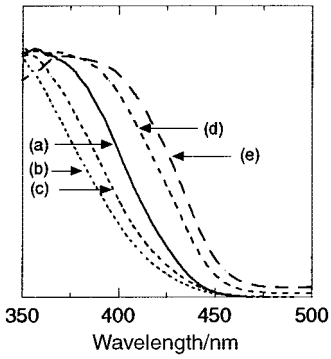

Fig. 7 Photoabsorption spectra of (a) HTT-WO_3 (WO_3-B) and WO_3 products obtained by calcination of Tungstite-B at (b) 873 K, (c) 973 K, (d) 1073 K and (e) 1173 K.

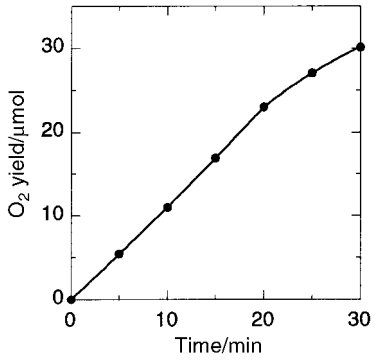

Fig. 8 Time course of O_2 evolution from Ag_2SO_4 in an aqueous suspension of WO_3-B under UV–visible light irradiation.

via IE-HTT showed higher activities than the commercial WO_3 samples; WO_3-B exhibited the highest activity. It has been pointed out that the crystallinity of TiO_2 controls the activity in photocatalytic O_2 evolution from an aqueous suspension of TiO_2.[11,12] The above-stated results clearly show that the same strategy of design can be applied to WO_3 photocatalysts for O_2 evolution. WO_3-C synthesized with a longer t_{HTT} possessed higher crystallinity and was expected to show higher activity than, for example, that of WO_3-B. However, this was not the case. As observed in SEM (Fig. 2), WO_3-C particles, unlike WO_3-B particles, were strongly coagulated to give large secondary particles. It is known that grain boundaries of TiO_2 particles induce recombination of electron–hole pairs.[27] Coagulation of particles might produce crystal defects, at boundaries of WO_3 particles, acting as recombination centers of electron–hole pairs. WO_3-G prepared from Tungstite-B by HTT showed a smaller O_2 yield than those of other HTT and commercial WO_3 samples. The crystallinity of this WO_3 powder might be too low for O_2 formation; this low crystallinity is suggested by its relatively large S_{BET} ($8.9\ m^2\ g^{-1}$) as discussed in the previous section.

WO_3 was also prepared from Tungstite-B by the calcination process. As shown in Fig. 9, the activities of these WO_3 samples obtained by calcination increased with elevation of T_C up to 973 K, due to the improved crystallinity of WO_3 upon calcination. A similar positive effect of calcination was also observed for WO_3-G, synthesized from Tungstite-B by HTT. The decrease in S_{BET} (Fig. 6) suggested that the crystallinity of the calcined WO_3 samples was improved. The activity of the samples obtained by calcination of WO_3-G was higher than that of the WO_3 sample obtained by direct calcination of Tungstite-B and was comparable to that of commercial WO_3-H. More severe calcination, however, decreased the activity of both WO_3 samples. It is well known

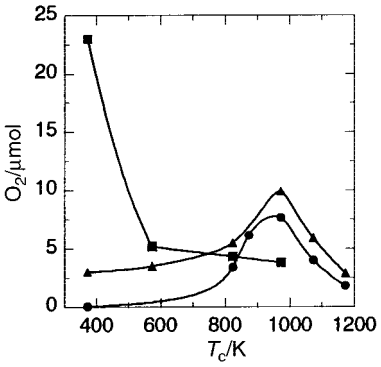

Fig. 9 Effects of calcination temperature on photocatalytic O_2 evolution from Ag_2SO_4 in aqueous suspensions of WO_3-B (■), WO_3-G (▲) and WO_3 derived from Tungstite-B (●).

that surface defects on TiO_2 particles act as recombination centers of electron–hole pairs, leading to a decrease in the photocatalytic activity of TiO_2.[27] Similarly, oxygen vacancies in and/or on WO_3 produced by calcination at $\geqslant 1073$ K may have induced recombination, resulting in a lower activity. Therefore the catalytic activity of WO_3 can be improved to some extent by calcination but only to a certain degree. On the other hand, HTT leads to WO_3 powders of high crystallinity without creation of oxygen vacancies, leading to much higher photocatalytic activity for O_2 evolution than for WO_3 samples prepared by calcination. Calcination of WO_3-B slightly reduced S_{BET} (Fig. 6) but drastically decreased the photocatalytic activity as shown in Fig. 9. It is well known that calcination induces aggregation of particles. WO_3-B particles were aggregated upon calcination, and surface defects were produced at grain boundaries of the particles, resulting in a decrease in the O_2 yield. The monoclinic WO_3 phase reversibly transforms to the orthorhombic phase at 623 K.[28] This reversible transformation in WO_3 might also produce crystal defects, thereby reducing the photocatalytic activity of the calcined WO_3-B samples.

Photocatalytic activity was also examined with 2 h photoirradiation at a wavelength of >420 nm using a cut-off filter. WO_3-B gave 12 μmol yield of O_2 under visible-light irradiation, though the apparent activity was much smaller than that with UV–visible irradiation due to the large decrease in the total number of photons irradiated on the WO_3 particles. Degussa P-25, one of the most active TiO_2 photocatalysts, showed negligible O_2 evolution (0.3 μmol) due to the larger band gap energy (3.2 eV corresponding to *ca.* 390 nm).

Conclusions

The results obtained in this study have shown that HTT is effective for synthesizing WO_3 photocatalysts of high activity for the formation of O_2 under deaerated conditions. HTT-WO_3 samples of high crystallinity, especially those prepared from an H_2WO_4 solution, exhibited higher O_2 evolution activity than did commercial WO_3 samples, indicating that the crystallinity of WO_3 is a decisive factor in the activity for O_2 evolution. WO_3 was also obtained by calcination of solid H_2WO_4 samples, and the crystallinity was improved to some extent by calcination at a high temperature, but more severe calcination conditions decreased the activity, probably due to the formation of oxygen vacancies.

References

1 J. R. Darwent and A. Mills, *J. Chem. Soc., Faraday Trans. 2*, 1982, **78**, 359.
2 W. Erbs, J. Desilvestro, E. Borgarello and M. Grätzel, *J. Phys. Chem.*, 1984, **88**, 4001.
3 K. Sayama and H. Arakawa, *J. Phys. Chem.*, 1993, **97**, 531.
4 T. Ohno, F. Tanigawa, K. Fujihara, S. Izumi and M. Matsumura, *J. Photochem. Photobiol. A: Chem.*, 1998, **118**, 41.
5 *Photocatalysis: Fundamentals and Applications*, ed. N. Serpone and E. Pelizzetti, Wiley, 1989.
6 A. Fox and M. T. Dulay, *Chem. Rev.*, 1993, **93**, 341.
7 M. R. Hoffmann, S. T. Martin, W. Choi and D. W. Bahnemann, *Chem. Rev.*, 1995, **95**, 69.
8 T. Watanabe, A. Kitamura, E. Kojima, C. Nakayama, K. Hashimoto and A. Fujishima, in *Photocatalytic Purification and Treatment of Water and Air*, ed. D. E. Ollis and H. Al-Ekabi, Elsevier, 1993. p. 747.
9 H. Kominami, Y. Takada, H. Yamagiwa, Y. Kera, M. Inoue and T. Inui, *J. Mater. Sci. Lett.*, 1996, **15**, 197.
10 H. Kominami, M. Kohno, Y. Takada, M. Inoue, T. Inui and Y. Kera, *Ind. Eng. Chem. Res.*, 1999, **38**, 3925.
11 H. Kominami, T. Matsuura, K. Iwai, B. Ohtani, S.-i. Nishimoto and Y. Kera, *Chem. Lett.*, 1995, 693.
12 H. Kominami, S.-y. Murakami, Y. Kera and B. Ohtani, *Catal. Lett.*, 1998, **56**, 125.

13 B. Ohtani, K. Iwai, H. Kominami, T. Matsuura, Y. Kera and S.-i. Nishimoto, *Chem. Phys. Lett.*, 1995, **242**, 315.
14 H. Kominami, J.-i. Kato, M. Kohno, Y. Kera and B. Ohtani, *Chem. Lett.*, 1996, 1051.
15 B. Ohtani, M. Masuoka, T. Atsumi, S.-i. Nishimoto and T. Kagiya, *Chem. Express*, 1988, **3**, 319.
16 B. Ohtani and S.-i. Nishimoto, *J. Phys. Chem.*, 1993, **97**, 920.
17 B. Ohtani, Y. Okugawa, S.-i. Nishimoto and T. Kagiya, *J. Phys. Chem.*, 1987, **91**, 3550.
18 S.-i. Nishimoto, B. Ohtani, H. Kajiwara and T. Kagiya, *J. Chem. Soc., Faraday Trans. 1*, 1983, **79**, 2685.
19 S.-i. Nishimoto, B. Ohtani, H. Kajiwara and T. Kagiya, *J. Chem. Soc., Faraday Trans. 1*, 1985, **81**, 61.
20 Y. Oosawa and M. Grätzel, *J. Chem., Soc. Faraday Trans. 1*, 1988, **84**, 197.
21 S. Sato, *Hyomen*, 1990, **28**, 427.
22 S. Sato and T. Kadowaki, *Denki Kagaku (Electrochemistry)*, 1989, **57**, 1151.
23 JCPDS card No. 35-0270.
24 JCPDS card No. 43-1035.
25 JCPDS Card No. 84-0886.
26 M. S. Farag, Z. Hanafi and M. A. Khilla, *Z. Phys. Chem. Neue Folge*, 1971, **76**, 265.
27 P. T. Landsberg, *Recombination in Semiconductors*, Cambridge University Press, Cambridge, 1991, p. 208.
28 B. L. Crowder and M. J. Sienko, *Inorg. Chem.*, 1965, **4**, 73.